

TUNNELING IN SINGLE-LAYER $\text{Bi}_2\text{Sr}_2\text{CuO}_{6+\delta}$ SINGLE CRYSTALS IN HIGH MAGNETIC FIELD

S. I. Vedeneev^{a,b,*}, *P. Szabó*^{b,c}, *A. G. M. Jansen*^b, *I. S. Vedeneev*^a

^a *P. N. Lebedev Physical Institute, Russian Academy of Sciences
117924, Moscow, Russia*

^b *High Magnetic Field Laboratory,
Max-Planck-Institut für Festkörperforschung/Centre National de la Recherche Scientifique
B. P. 166, F-38042 Grenoble Cedex 9, France*

^c *Institute of Experimental Physics, Slovak Academy of Sciences
SK-04353 Košice, Slovakia*

Submitted 25 December 2000

In the tunneling experiments with high-quality single crystals of single-layer cuprate superconductor $\text{Bi}_2\text{Sr}_2\text{CuO}_{6+\delta}$ using the break-junction and point-contact techniques at $T < T_c$, the coexistence of the superconducting-state gap and the normal-state gap was observed. The values of the superconducting energy gap $2\Delta_{p-p}$ are in the range 13.4–15 meV ($\Delta_{p-p} = 6.7\text{--}7.5$ meV). The values of $2\Delta_{p-p}$ are similar for two samples with $T_c = 4$ K and for two samples with $T_c = 9\text{--}10$ K and are independent of the carrier concentration. The normal-state gap, with the magnitude approximately equal to 50 meV, persists at $T < T_c$ and in the magnetic field $H \gg H_{c2}$ up to 28 T. After the transition of the sample to the normal state, the intensity of the tunneling conductance rapidly decreases with increasing magnetic field and temperature. The observed large broadening of the tunneling spectra and large zero-bias conductances can be caused by a strong angular dependence of the superconducting gap. The tunneling results are in full agreement with the angle-resolved photoemission spectroscopy measurements.

PACS: 74.72.Hs, 74.50.+r, 74.25.Jb

It is known that the tunneling spectroscopy has been used successfully in studying the superconducting state in conventional superconductors. However this method has encountered considerable difficulties in the case of high-temperature superconductors (HTSC) due to an extremely small coherence length ξ and high inhomogeneity of samples. At present, more reproducible results are only obtained for the bilayered cuprate $\text{Bi}_2\text{Sr}_2\text{CaCu}_2\text{O}_{8+\delta}$ (Bi2212). Previously [1, 2], we have performed an extensive tunneling study on high-quality Bi2212 single crystals using the break-junction technique. Our experiments show that the presently available quality of Bi2212 samples enables fabricating good-quality tunnel junctions in the *ab*-plane with a low or almost zero leakage current and a well developed gap structure in the tunneling spectra. The angle-resolved photoemission spectroscopy

(ARPES) measurements [3–6] have confirmed the energy gap value found but on the other hand, have given evidence to a strong angular dependence of the gap that is consistent with a four-lobed $d_{x^2-y^2}$ order parameter. In addition, many experiments (e.g. NMR [7], photoemission [5], and tunneling [8]) have provided evidence that in the normal state of the underdoped Bi2212, a pseudogap exists in the electronic excitation spectra at temperatures T^* above the superconducting transition temperature T_c . In scanning tunneling measurements on Bi2212, Renner et al. [8] have found this pseudogap to be present both in underdoped and overdoped samples, and to scale with the superconducting gap. It has been proposed that the pseudogap in the normal state can be seen as a precursor for the occurrence of superconductivity where the superconducting phase-coherence is suppressed by thermal or quantum fluctuations [9–11]. In the case of a nonsuperconduct-

*E-mail: vedeneev@sci.lebedev.ru

ing origin, the pseudogap can be formed in the spin part of the excitation spectrum.

The situation for the low- T_c single-layer cuprate superconductor $\text{Bi}_2\text{Sr}_2\text{CuO}_{6+\delta}$ (Bi2201) is more complicated. The first point contact tunneling measurements of the superconducting energy gap in imperfect Bi2201 crystals were performed long ago [12]; up to now, however, it has been impossible to fabricate a high-quality tunnel junction using the break-junction method. Because the coherence length ξ_{ab} in Bi2201 is larger than in Bi2212 and reaches 45 Å [13], it is very difficult to prepare directly a quality tunnel barrier in a liquid helium. In ARPES experiments, Harris et al. [14] have observed highly anisotropic superconducting gaps of 10 ± 2 and 7 ± 3 meV in the optimally doped and the underdoped $\text{Bi}_2\text{Sr}_{2-x}\text{La}_x\text{CuO}_{6+\delta}$ (Bi,La2201), respectively. They have also found a pseudogap above T_c and assumed that these two energy gaps can have a common origin in the pairing interaction. However, on the basis of the experimental study of the c -axis resistivity ρ_c in the normal state of nondoped Bi2201 single crystals under continuous high magnetic fields, we recently concluded [15] that superconductivity is probably not at the origin of the pseudogap. The tunneling study of high- T_c superconductors in the normal state under high magnetic fields can give important information on the nature of the pseudogap.

In this paper, we describe the tunneling measurements for several high-quality $\text{Bi}_2\text{Sr}_2\text{CuO}_{6+\delta}$ single crystals with midpoint $T_c = 3.5$ –4 K (overdoped) and 9–10 K (near optimally doped) using the break-junction and point-contact techniques under continuous magnetic fields H up to 28 T. A low T_c value for these crystals permits us to investigate the gap structures of a cuprate superconductor in the normal state down to low temperatures. In magnetic fields, we observed a different behavior of the superconducting and normal-state gaps. The previous results of the tunneling study using the break junction in lower magnetic fields were published in [16]. However, here we give a selection of these results because later magnetotransport measurements [13] allow us to understand an unusual behavior of differential conductances dI/dV in magnetic fields.

The Sr-deficient $\text{Bi}_{(2+x)}\text{Sr}_{2-(x+y)}\text{Cu}_{(1+y)}\text{O}_{6+\delta}$ single crystals with the Bi/Sr ratio of 1.4–1.5 for samples with $T_c = 9$ –10 K and 1.7 for samples with $T_c = 3.5$ –4 K (with the Bi excess localized at the Sr positions) were grown in a gaseous phase in closed cavities of the KCl-solution-melt [17]. Because of a long growing time, the single crystals have a high cation ordering. The crystal sizes are around $(0.5$ – $2.5)$ mm \times $(0.4$ – $2)$ mm \times $(1.5$ – $5)$ μm . The

half-widths of main reflections in X-ray rocking curves for single crystals do not exceed 0.1–0.3°, which is the minimum value reported so far. The crystal lattice parameters are $a = 5.353$ – 5.385 Å and $c = 24.600$ – 24.638 Å, and the superlattice periodicity is $\tilde{a} = 4.75a$. The superconducting transition width defined by 10% and 90% of the superconducting transition points ranges from 0.5 to 1.5 K. The onset temperatures in the superconducting transition for the dc -resistance and ac -susceptibility are close, and the transition widths are almost the same. The in-plane resistivity ρ_{ab} of the crystals shows a linear temperature dependence at high temperatures and saturates to the residual resistivity below 20–40 K. The in-plane resistivities slope $\Delta\rho_{ab}/\Delta T = 0.5$ – 1.5 $\mu\Omega\cdot\text{cm}/\text{K}$ was obtained at high temperatures. The residual resistivity $\rho_{ab}(0)$ is between 80 and 180 $\mu\Omega\cdot\text{cm}$. By measuring the normal-state Hall coefficient in our crystals in the temperature region of 4.2–50 K, we have found that the concentration of the carriers equals $n = (4.8$ – $6.3) \cdot 10^{21}$ cm^{-3} . The carrier density in low- T_c samples was larger than in the samples with $T_c = 9$ –10 K. It is believed [18] that single crystals of pure Bi-excess Bi2201 phase are always overdoped because Bi gives some intrinsic doping. This is reasonable if one considers the optimally La-doped Bi2201 polycrystal samples with the maximum for Bi2201 value $T_c \approx 25$ K and the carrier density $n \approx 3 \cdot 10^{21}$ cm^{-3} [18]. Our single crystals with $T_c = 3.5$ –4 K must therefore be assigned to heavily overdoped ones. On the other hand [19], the carrier concentrations in the underdoped Bi,La2201 single crystals with $T_c = 13$ K are similar. Because the magnitude of T_c in nondoped Bi2201 single crystals approximately equals 13 K, the samples with $T_c = 9$ –10 K studied here are most likely to be slightly underdoped or nearly optimally doped. The tunneling junctions were made *in situ* at 1.5 K by the break-junction superconductor/insulator/superconductor (SIS type) [2] or the tunnel point contact superconductor/insulator/normal metal (SIN type) [12], using Cu needle as a counter electrode. The current–voltage (I – V) characteristics and derivatives dV/dI were measured by the usual phase-sensitive detection technique. The tunneling in the break-junction geometry used in our experiments is supposed to probe the superconducting state in the ab plane [2].

The typical differential conductances dI/dV as functions of V for four break-junctions at $T = 2.6$ and 1.6 K for two single crystals (Nos. 1 and 2) with $T_c = 3.5$ and 4 K are shown in Fig. 1. Although the measurements were carried out at low (≈ 0.2 k Ω ,

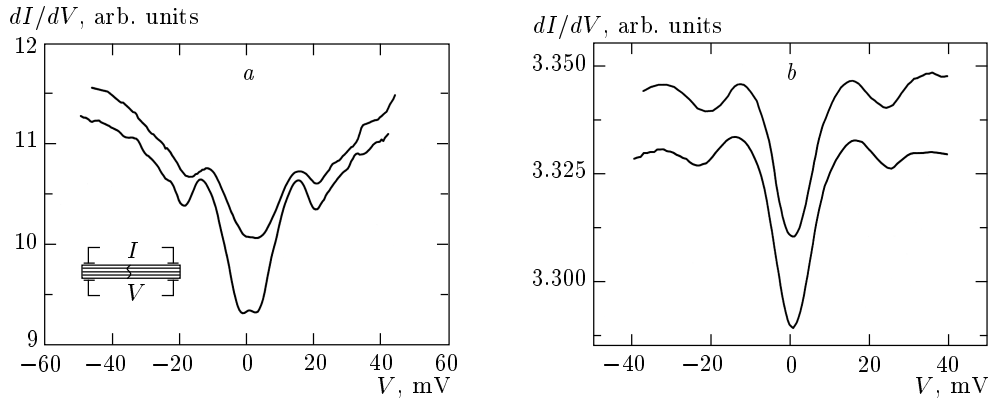


Fig. 1. Differential conductances dI/dV as functions of V for four break-junctions at (a) $T = 2.6$ K and (b) $T = 1.6$ K for Bi2201 single crystals (a) No. 1 and (b) No. 2 with $T_c = 3.5$ and 4 K, respectively. For clarity, the curves are shifted vertically with respect to the lower curves. The inset shows the geometry of the break junction

Fig. 1a) and moderately high (≈ 0.5 k Ω , Fig. 1b) resistances of the tunnel barrier, the spectra reveal a very large zero-bias conductance (80–90% of the conductance), the gap structure is strongly smeared and the conductance of the low-resistance junctions (Fig. 1a) has the V-shaped background. We have not observed anything similar in the tunneling experiments with Bi2212 single crystals [1, 2]. Recently, Mallet et al. [20] analyzed in detail the influence of different channels of a current leakage on the tunneling spectra of HTSC and suggested some correction procedure in order to extract the real tunneling density of states. However, in the given case, the zero-bias conductance is too large to be completely ascribed to the leakage current. In spite of numerous attempts, we could not obtain the curves of dI/dV versus V with the same clear gap structure and small zero-bias conductance as for Bi2212. Taking this circumstance into account, it seems that the large zero-bias conductance and strongly smeared gap structure in the tunneling spectra in Fig. 1 are more probably related to a high anisotropy of the superconducting gap in Bi2201 observed recently in ARPES experiments by Harris et al. [14]. In the underdoped Bi,L a2201 single crystals, they observed not sharp, but a reproducible gap of 7 ± 3 meV along the $(\pi, 0)$ symmetry line of the \mathbf{k} -space and a zero gap at 45° . For the SIS junctions studied here, the peak-to-peak distance between two main maxima on the dI/dV curves must correspond to $4\Delta_{p-p}$. As can be seen in Fig. 1, the value of the superconducting energy gap $2\Delta_{p-p}$ is in the range of 13.4–15 meV (with $\Delta_{p-p} = 6.7$ –7.5 meV). The break-junction method is a technique probing the tunneling density of states integrated over the polar angle in the k_{ab} -space. The strong angular dependence of the en-

ergy gap with zero value in some directions must result in a high density of states inside the gap [20] (large zero-bias conductance in tunneling spectra) and to a strongly smeared gap structure corresponding to the upper limit of Δ_{p-p} . This is in full agreement with the ARPES measurements [14]. Both our tunneling spectra and ARPES spectra have a broad gap structure that is difficult to describe within a simple BCS model. We have only used the phenomenological parameter Γ to take the pair breaking effects into account [21] and obtained the energy gap of 3.5–4 meV that is very close to that measured by us in the point-contact tunneling experiments on Bi2201 [12].

To prove a relation between the energy gap and T_c , we have measured the tunneling conductances dI/dV at different temperatures shown in Fig. 2. It can be seen that the gap structure (marked by arrows) broadens and diminishes as the temperature increases with a small decrease in the feature position. Because $T_c = 4$ K for the given sample and the gap structure disappears at T near T_c , we can assume that the observed energy gap is definitely the superconducting state gap of Bi2201. Because the gap structure is smeared out and the zero-bias conductance is high, it is impossible to investigate the temperature dependence of the superconducting gap in detail.

The tunneling spectrum of the superconductor outside the gap for high-Ohmic junctions with a good tunneling barrier is known to be flat [22] because this is expected for a Fermi liquid. The V-shaped form of the conductance for the low-resistance junctions comes from the bias voltage-induced barrier decreasing. However, the results in Fig. 2 show that the form of the background changes from flat to V-shaped with an in-

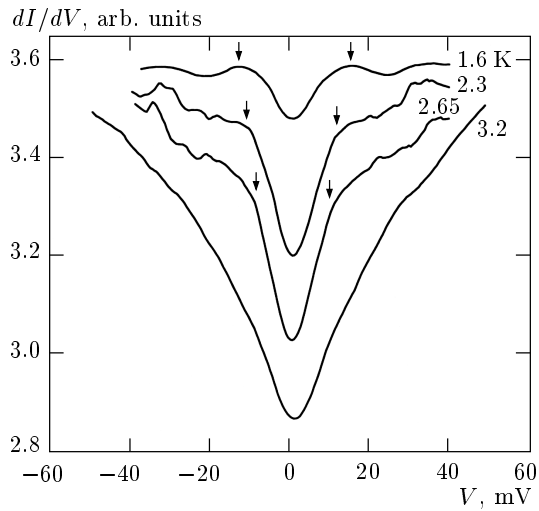


Fig. 2. Tunneling conductances dI/dV versus V at different temperatures for sample No. 2. The curves are shifted with respect to the upper one. The gap structure is marked by arrows

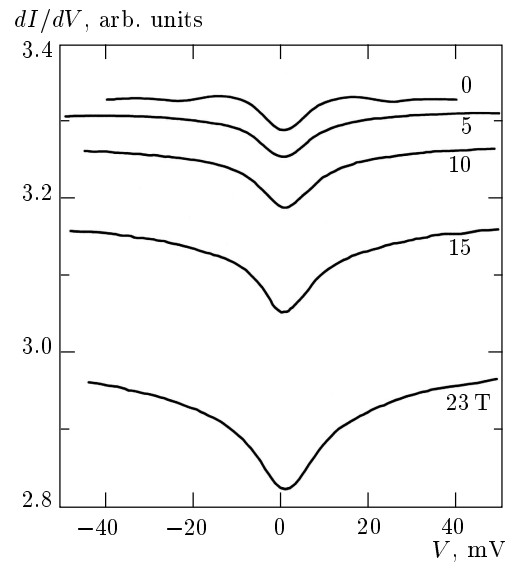


Fig. 3. The effect of the magnetic field on tunneling conductances dI/dV as functions of V at $T = 1.4$ K (\mathbf{H} is parallel to the c -axis), sample No. 2

creasing temperature. Moreover, the V-shaped background conductance increases remarkably with an increasing temperature. One of the reasons for the observed change can be a temperature-induced barrier damping or the temperature dependence of the coherence length ξ . Near T_c , ξ is large and the measured tunneling density of states is determined not only by the CuO_2 planes but also by the nonmetallic Bi-O layers. To exclude the influence of the temperature-induced barrier transparency change, we have measured the tunneling spectra of the break-junction in magnetic fields above the upper critical field H_{c2} at a given temperature in the geometry when \mathbf{H} is parallel to the c -axis.

The effect of the magnetic field on the tunneling conductance dI/dV at $T = 1.4$ K is shown in Fig. 3. As can be seen, the behavior of the Bi2201 break-junction in magnetic field sharply differs from that for Bi2212 [1, 2]. First, the magnitude of the tunnel-junction conductance decreases with increasing magnetic field and the curves of dI/dV versus V significantly shift down, thereby decreasing the zero-bias conductance. Second, in the magnetotransport experiments [13] carried out after the tunneling measurements [16], we have found that the ab -plane H_{c2} in our low- T_c Bi2201 single crystals equals 10 T at $T = 1.4$ K but the gap structure in Fig. 3 practically disappears already at 5 T. As was mentioned above, the tunnel current probes a region of the order of the coherence length. For the break-junction in the mixed state, the

conductance dI/dV corresponds to the tunneling density of states for an isolated vortex with a normal core and the superconducting density of states near the vortex is broadened by the pair-breaking effect of the local magnetic field. Thus, the superconducting gap structure can be already smeared at $H \ll H_{c2}$. We note that the barrier transparency at constant temperature remains unchanged and the general form of tunneling conductances is preserved. In the tunneling measurements of the conventional superconductors in magnetic fields $H > H_{c2}$, the differential conductance dI/dV is constant at eV from zero to Δ . In the present case, a large dip around $V = 0$, seen in Fig. 3, indicates the existence of an energy gap in high magnetic fields up to 23 T. Although the spectra are so broad that it is difficult to define the gap value exactly, we can say that this gap persists even in the normal state at $H \gg H_{c2}$. At the same time, we found that the V -dependences of the differential resistance dV/dI at two points with $V = 0$ and 40 mV extracted from Fig. 3 are quadratic in the magnetic field in a wide range of fields without the saturation occurring for the classical magnetoresistivity of a normal metal in the transverse configuration. The data in Fig. 3 point out that, due to a large anisotropy of the resistance of Bi2201 single crystals ($\rho_c/\rho_{ab} \sim 10^3\text{--}10^4$ [13]), the measurement current in the break-junction geometry flows in a very thin layer of the sample. In high magnetic fields, the resistance of this near-barrier region can be of the or-

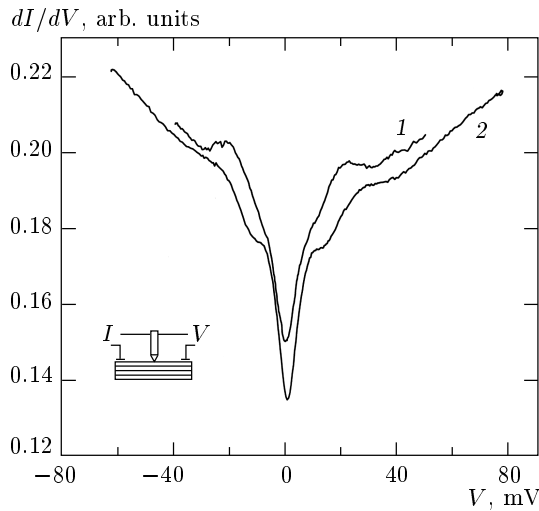


Fig. 4. Differential conductances dI/dV versus V for Bi2201–Cu tunnel point contacts fabricated on single crystals No.24 (curve 1) and No.44 (curve 2) with $T_c = 9$ and 10 K, respectively ($T = 1.6$ K, $H = 0$, $R_t = 0.6$ k Ω). The inset schematically shows the geometry of the point contact

der of or larger than the resistance R_t of the tunneling barrier. In this case, the break junction is not quite a four-probe junction, and the applied voltage drops partially across the bulk of the crystal and not only across the tunneling barrier, especially at low temperatures, where the nonmetallic resistance along the c -axis becomes very large.

To partially exclude the influence of the crystal resistance on the measured tunneling spectra, we have studied the point-contact tunnel junctions in which the four-probe contact method can be better realized. The tip of a copper wire needle was pressed perpendicularly to the crystal surface (parallel to the c -axis). The magnetic field was also oriented parallel to the c -axis. The point-contact tunnel junctions use the natural oxide layer on the contact-forming electrodes as a tunneling barrier. In our experiments, the point contacts revealed a high resistance after the first touch in liquid helium at 1.5 K; the background conductance was only increasing with increasing bias voltage. After a further increase of the pressure applied to the tip, a gap-like structure appeared in the I – V characteristics of the contacts.

The differential conductances dI/dV of Bi2201–Cu tunnel point contacts fabricated on two single crystals, Nos. 24 and 44, with $T_c = 9$ and 10 K, respectively, are shown in Fig. 4. The tunneling barrier resistance R_t for these contacts at $T = 1.6$ K is equal to about 0.6 k Ω . The gap structure on the characteristics of the SIN-

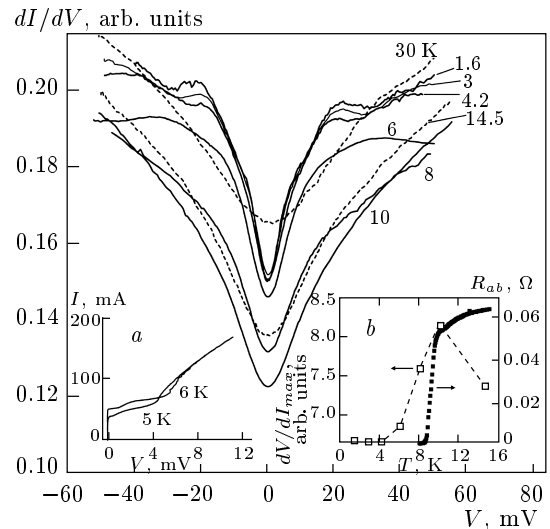


Fig. 5. Differential conductances dI/dV as functions of V for Bi2201–Cu tunnel point contacts at different temperatures (sample No.24, $H = 0$). Inset a shows the I – V characteristics of the tunnel break junction with a very low resistance ($< 0.1\Omega$) fabricated from the same single crystal where the superconducting energy gap is well seen at 6 K. In inset b , we have plotted the temperature dependence of the differential resistance dV/dI at $V = 0$ extracted from the experimental data in combination with the ab -plane superconducting transition curve of the given single crystal

type tunnel junctions is always smeared larger than in the case of SIS-type junctions. Nevertheless, the zero-bias conductance for our point-contact tunnel junctions was less than for the break junctions. Two pairs of symmetric features on the curves plotted in Fig. 4 can be easily seen, and we believe to have observed two energy gaps. The peak-to-peak distances between the symmetric maxima on the curves of dI/dV versus V lie in the range of 15–18 and 45–50 mV. The magnitude of the first gap is in close agreement with data in Fig. 1 although the T_c value of the given crystal is nearly twice as that of crystal No. 2 in Fig. 1. The second pair of gap features in the SIS break junctions in case of a true gap must be located near 100 mV ($4\Delta_{p-p}$), which we did not study for break junctions.

In Fig. 5, we have plotted the differential conductances dI/dV for the Bi2201–Cu tunnel point contact at different temperatures. It can be seen that the gap structure again broadens and rapidly vanishes with increasing temperature. At low temperatures away from T_c , the tunneling barrier transparency does not change because the conductance spectra shapes are preserved. However, starting from $T \geq 5$ K, the V -shaped back-

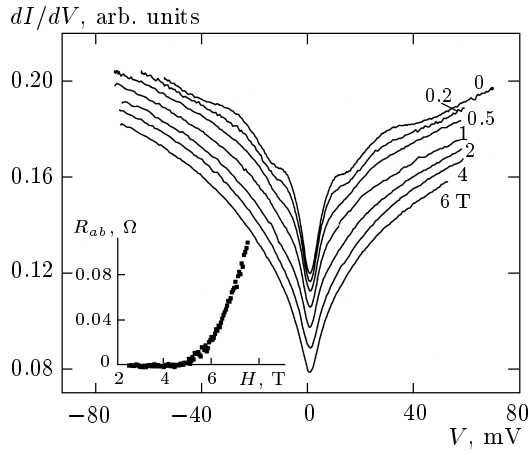


Fig. 6. Differential conductances dI/dV as functions of V for the Bi2201–Cu tunnel point contacts at $T = 1.6$ K and for different values of the field oriented along the c -axis of the crystal (No. 44). The curves are shifted vertically by the same value with respect to the $H = 0$ curve. The inset shows the ab -plane resistance of the same Bi2201 crystal

ground conductance slightly enhances with increasing temperature, the differential conductances at zero bias $V = 0$ change, and the curves shift down. Since $T_c = 9$ K for the given sample (No. 24), the gap structure is believed to vanish at $T < T_c$, but this is not the case. Inset *a* in Fig. 5 shows I – V characteristics of the low-resistance ($< 0.1 \Omega$) tunnel break junction fabricated from the same single crystal where the superconducting energy gap is well seen at 6 K. In inset *b* in Fig. 5, we have plotted the temperature dependence of the differential resistance dV/dI at $V = 0$ extracted from the experimental data in combination with the ab -plane superconducting transition curve of the given single crystal. It is easy to verify that the crystal resistance rise and the shift of the dI/dV curves in Fig. 5 with an increasing temperature are caused by the superconducting transition of the Bi2201 crystal region near the tunneling barrier as before even if $R_t \approx 0.6$ k Ω . The tunneling conductance behavior at temperatures near and above T_c for the point contacts (Fig. 5) is identical to that for break junctions (Fig. 2).

The effect of the magnetic field on the gap structure at $T = 1.6$ K is illustrated in Fig. 6, where we show the differential conductances dI/dV for the Bi2201–Cu tunnel point contact at different fields oriented along the crystal c -axis ($R_t \approx 0.6$ k Ω). In moderate magnetic fields (up to 6 T), the dI/dV curves did not shift with respect to each other; for clarity, the curves in Fig. 6 have been shifted vertically by the same value

with respect to the $H = 0$ curve. As earlier, the gap features broaden and practically diminish already at 4 T, although the respective values of T_c and ab -plane H_{c2} at 1.6 K are equal to 10 K and 22 T for crystal No. 44. In the point junction region of the crystal, additional pinning centers are produced by the pressure between the contact-forming electrodes. In this case, the tunneling conductance dI/dV mainly conforms to the density of states in the normal vortex cores near the contact already at $H > H_{c1}$. As is illustrated by the inset in Fig. 6, the ab -plane resistance of the same Bi2201 crystal in magnetic field 4 T still equals zero, but the gap structure is hardly visible.

A steady value and the general shape of the conductance spectra in the magnetic field up to 6 T made it possible to normalize the last dI/dV curves at $H = 0$ –5 T by the conductance at $H = 6$ T, where the gap structure is no longer visible, in order to see the magnetic field influence on the gap features more clearly. In the normalized conductances, the gap structure broadens and diminishes gradually at increasing fields with a decrease in peak positions. The peak-to-peak distance between the two main maxima of the dI/dV curve at $H = 0$ is equal to 14.8 mV ($\Delta_{p-p} = 7.4$ meV). As noted above, this value is coincident with that measured by the break-junction technique. It is surprising that the magnitude of $2\Delta_{p-p}$ is similar for two samples with $T_c = 4$ K and two samples with $T_c = 9$ –10 K and is independent of the carrier concentration. So far as our normalization is not quite correct, it is difficult to give a quantitative analysis of the magnetic field effect on the gap value. However, the shift in the position of the features in the normalized conductance in Fig. 6 reflects the reduction of the order parameter in the point-contact region in the magnetic field. It is reasonable to expect that there are additional pinning centers in the point junction region of the crystal, and hence, the number of fixed vortices rapidly increases with the magnetic field. This leads to a fast suppression of the order parameter and the closing of the superconducting energy gap in the magnetic field $H \ll H_{c2}$.

The second pair of maxima in the upper part of the dI/dV curves in Figs. 4–6 is related to the large dip around zero voltage, the main shape of which does not vary with the magnetic field and temperature. The peak-to-peak distance between the second maxima in zero field is approximately equal to 52 mV. As the main maxima, these maxima broaden with increasing magnetic field, but the shift in the position of peaks in the normalized conductances is only slight. This gap does not close above T_c and H_{c2} , as indicated by Figs. 3

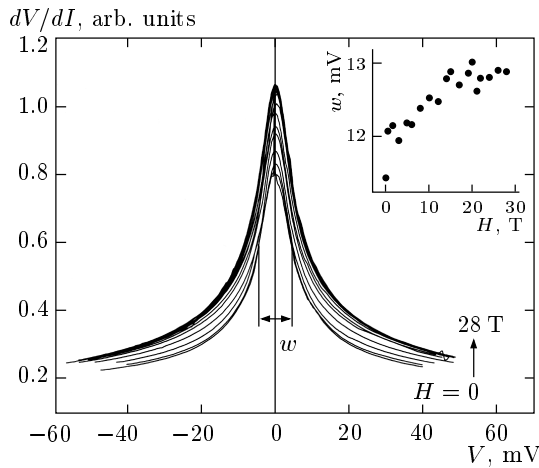


Fig. 7. Differential resistances dV/dI as functions of V for $\text{Bi}2201\text{-Cu}$ contacts at 1.6 K in different magnetic fields (sample No. 44, $R_t = 4.5 \text{ k}\Omega$, $T = 1.6 \text{ K}$), \mathbf{H} is parallel to the c -axis. A variation of the half-width of the gap versus magnetic field is shown in the inset

and 5, and can be identified with the normal-state gap of $\text{Bi}2201$ observed in ARPES experiments by Harries et al. [14]. Because this gap occurring in the tunneling spectra is so broad and the zero-bias conductance is so large, there is a non-zero state density at the Fermi energy, i.e., the true gap does not exist [5]. Our point-contact tunneling spectra at low temperatures and zero magnetic field can be presumably described by a representative background, two broad peaks near the energies $\pm 25 \text{ meV}$, and sharper peaks at the energies $\pm 7.4 \text{ meV}$, as was done in ARPES experiments with $\text{Bi}2212$ [6].

Next, we studied the magnetic field dependence of the normal-state gap in more detail using a sufficiently high-Ohmic point-contact tunnel junction with $R_t = 4.5 \text{ k}\Omega$. Such large resistance makes the observation of the superconducting gap difficult but ensures only a negligible effect of the crystal magnetoresistance on the main shape of the tunneling spectra. Figure 7 shows the series of the differential resistances dV/dI as functions of V for this $\text{Bi}2201\text{-Cu}$ contact at 1.6 K in different magnetic fields. It can be seen that the shape of the tunneling spectra does not vary with the magnetic field and the data provide clear evidence that the normal-state gap still exists up to 28 T. A variation of the half-width of the gap versus magnetic field is shown in the inset in Fig. 7. In Fig. 8, we have plotted the magnetic field dependences of the zero-bias differential resistances dV/dI at $T = 1.6, 4.2$, and 10 K normalized to the corresponding maximum values. Here, we

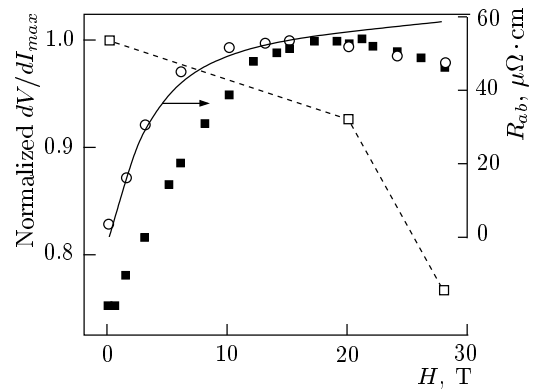


Fig. 8. The magnetic field dependences of the zero-bias differential resistances dV/dI at temperatures 1.6 K (full squares), 4.2 K (circles), and 10 K (open squares) normalized to the respective maximum values. The solid line shows the ab -plane superconducting transition of the same crystal in the magnetic field at 4.2 K

also show the ab -plane superconducting transition of the same crystal in the magnetic field at 4.2 K (solid line). From Fig. 8 and the inset in Fig. 7, it is clear that the transition of the sample to the normal state is responsible for a small increase in the gap half-width and the enhancement of the differential resistance at $V = 0$. However, after the transition of the sample to the normal state, the intensity of the dV/dI curves (the dip amplitude in tunneling conductance) starts to decrease rapidly with the magnetic field. Furthermore, we note that the intensity of the tunneling spectra at $V = 0$ also undergoes a rapid decline at $T > T_c$. This is in contrast with heavily underdoped $\text{Bi}2212$ samples with $T_c = 10 \text{ K}$ [5], where the large normal-state gap does not close even at 301 K. Our last result agrees well with the data of ARPES measurements of optimally doped $\text{Bi}2212$ [6].

It is probable that the normal-state gap observed in tunneling experiments is the pseudogap that has been widely discussed recently. It is worth mentioning that many tunneling conductances with a similar shape and a large dip in the vicinity of the zero-bias voltage have been observed in the metal/insulator/semiconductor tunnel junctions [23]. In particular, the conductance peaks and a large dip on the tunneling spectra of the Bi-alloy junction [24] were attributed to the energy gap and to the band bending near the surface due to the applied voltage, respectively. It is interesting that with an increasing magnetic field, the conductance peaks tend to be washed away whereas the dip due to the energy gap is deepened. Therefore, it is quite possible that a

normal gap in BiO layers manifests itself in our measurements as the large dip near the zero-bias voltage.

To summarize, in the tunneling experiments with high-quality single crystals of single-plane Bi2201 cuprate superconductor using the break-junction and point-contact techniques at $T < T_c$, we observed the coexistence of the superconducting-state gap and the normal-state gap. The value of the superconducting energy gap $2\Delta_{p-p}$ is in the (13.4–15)-meV range ($\Delta_{p-p} = 6.7\text{--}7.5$ meV). The values of $2\Delta_{p-p}$ are similar for two samples with $T_c = 4$ K and two samples with $T_c = 9\text{--}10$ K and are independent of the carrier concentration. At $T < T_c$, the normal-state gap with the magnitude approximately equal to 50 meV persists in the magnetic field $H \gg H_{c2}$ up to 28 T. However, after the transition of the sample to the normal state, the intensity of the dV/dI versus V curves (the dip amplitude in the tunneling conductance) starts to decrease rapidly with the increasing magnetic field and temperature. The observed large broadening of the tunneling spectra and large zero-bias conductances can be caused by a strong angular dependence of the superconducting gap. The tunnel results are in full agreement with the angle-resolved photoemission spectroscopy measurements [14].

One of the authors (S. I. V.) was partially supported by the Russian Ministry of Science and Technical Policy under the Program for Actual Problems in Condensed Matter Physics (grant No. 96001) and by the Russian Foundation for Basic Research (project No. 99-02-17877).

REFERENCES

1. S. I. Vedeneev, K. A. Kuznetsov, V. A. Stepanov et al., *Pis'ma Zh. Eksp. Teor. Fiz.* **57**, 338 (1993) [*JETP Lett.* **57**, 352 (1993)].
2. S. I. Vedeneev, A. G. M. Jansen, P. Samuely et al., *Phys. Rev. B* **49**, 9823 (1994).
3. J. M. Harris, Z.-X. Shen, P. J. White et al., *Phys. Rev. B* **54**, 15665 (1996).
4. D. S. Marshall, D. S. Dessan, A. G. Loeser et al., *Phys. Rev. Lett.* **76**, 4841 (1996).
5. H. Ding, T. Yokoya, J. C. Campuzano et al., *Nature (London)* **382**, 51 (1996).
6. A. V. Fedorov, T. Valla, P. D. Johnson et al., *Phys. Rev. Lett.* **82**, 2179 (1999).
7. C. Berthier, M.-H. Julien, O. Bakharev et al., *Physica C* **282–287**, 227 (1997).
8. Ch. Renner, B. Revaz, J.-Y. Genoud et al., *Phys. Rev. Lett.* **80**, 149 (1998).
9. V. Emery and S. A. Kivelson, *Nature (London)* **374**, 434 (1995).
10. T. Hotta, M. Mayr, and E. Dagotto, *Phys. Rev. B* **60**, 13085 (1999).
11. J. Maly, B. Jankó, and K. Levin, *Phys. Rev. B* **59**, 1354 (1999).
12. S. I. Vedeneev, P. Samuely, A. G. M. Jansen et al., *Z. Phys. B–Condens. Matter* **83**, 343 (1991).
13. S. I. Vedeneev, A. G. M. Jansen, E. Haanappel et al., *Phys. Rev. B* **60**, 12467 (1999).
14. J. M. Harris, P. J. White, Z.-X. Shen et al., *Phys. Rev. Lett.* **79**, 143 (1997).
15. S. I. Vedeneev, A. G. M. Jansen, and P. Wyder, *Phys. Rev. B* **62**, 5997 (2000).
16. S. I. Vedeneev, *Pis'ma Zh. Eksp. Teor. Fiz.* **68**, 217 (1998) [*JETP Lett.* **68**, 230 (1998)].
17. V. P. Martovitsky, J. I. Gorina, and G. A. Kaljuzhnaia, *Sol. St. Comm.* **96**, 893 (1995); J. I. Gorina, G. A. Kaljuzhnaia, V. P. Martovitsky et al., *Sol. St. Comm.* **108**, 275 (1998).
18. A. Maeda, M. Hase, I. Tsukada et al., *Phys. Rev. B* **41**, 6418 (1990).
19. Y. Ando, G. S. Boebinger, A. Passner et al., *Phys. Rev. B* **56**, 8530 (1997).
20. P. Mallet, D. Roditchev, W. Sacks et al., *Phys. Rev. B* **54**, 13324 (1996).
21. R. C. Dynes, V. Narayanamurti, and J. P. Garno, *Phys. Rev. Lett.* **41**, 1509 (1978).
22. K. Kitazawa, *Science* **271**, 313 (1996).
23. E. L. Wolf, *Principles of electron tunneling spectroscopy*, Oxford University Press, New York (1985).
24. L. Esaki and P. J. Stiles, *Phys. Rev. Lett.* **16**, 574 (1966).